A 50 Hz Solar Powered D.C. To A.C. Inverter.

Martin C.O. O'Bryan.

NEG 490 Electrical Engineering Honours Thesis.

A 50 Hz Solar Powered D.C. to A.C. Inverter.

Martin C.O. O'Bryan.

Martin C.O. O'Bryan.

October 1990.

This thesis is submitted in partial fulfilment of the requirements of the Degree of Bachelor of Engineering with Honours at the University of Tasmania.

Abstract.

This thesis describes the steps taken for the design and testing of a 50 Hz solar powered DC to AC inverter. The inverter has two modes of operation. The first mode will link the output of the inverter across the mains, assisting the mains to supply a load. The second mode of operation should be capable of supplying a load, independent of the mains supply. The batteries used to power the inverter would be kept charged up by use of solar panels.

Acknowledgments.

I would like to express my gratitude to the following people for their help and support during the duration of my honours.

Many thanks to Mr John Kan for partnering me for this design project.

Many thanks to Mr J. Brodie for his enthusiastic supervision of the design. Both John and I are most grateful for his encouragement and confidence throughout the year.

To Mr. R. Langman for all the times he assisted us, especially in regard to the design of the transformer and inductors.

To Mr. Steve Avery for his technical assistance and perseverance.

To Mr. Grace and Mr. R. Wherrett for their incidental help.

To Paul Holloway for time he spent proof reading this thesis and for the overextended loan of the Macintosh that allowed it to be typed.

To all my fellow fourth year Elecs (and even the computer heads). Thank you for your humour, support, comradeship and car lifts especially in the last two years.

To all my friends, from the Engineering Faculty, from college and others, for making the last four years as enjoyable as they have been.

Special thanks to all my family for their tremendous support over the total duration of my degree and education.

Contents.

An Introduction.

The aim of this design was to convert power from D.C. batteries, that are charged from solar cells, to A.C. power required by a 240 V_{rms} 50 Hz load. The design has two main modes of operation, firstly to assist the mains to supply power to a load and secondly to power a load independent of the mains supply.

The design can be classified into three main parts.

1.) The Parallel Inverter.
2.) The Filter.
3.) The Control Circuitry required to control the switching of the inverter's transistors.

The parallel inverter consists of a toroidal cored transformer with a centre tapped primary winding and transistors which provide the switching. Feedback diodes were included due to large L*di/dt components that were created by the switching of the transistors. It was the aim of these diodes to restrain the voltage produced across either of the primary windings from exceeding the supply voltage from the battery. These diodes also helped to maintain a square wave output across the primary of the transformer.

The filter was based on a combination of two resonant circuits, one a series circuit, the other parallel. Both these circuits are resonant at 50 Hz. The filter was required to have a bandwidth of between 48 Hz and 52 Hz, the quoted mains variance in frequency. Other requirements are that the filter's operation should be independent of the load, as well as not dissipating power.

The control circuitry is split into two parts, one for each mode of operation. The mains assisting mode control circuitry is based on a method that controls the phase between the inverter output and the mains and consists of three main parts.

1.) The Phase Circuit.
2.) A Zero-Crossing Detector.
3.) The Drive Circuit.

The independent mode of operation required a 50 Hz oscillation. This oscillation was successfully achieved by the use of a circuit using three inverters and a resistor, capacitor combination.

CHAPTER ONE:

Basic Discussion on Inverters.

1.1 Choice Between the Series and Parallel Inverter.

It is the role of the inverter to make the conversion from the Direct Current (D.C.) source of the batteries to an Alternating Current (A.C.) source that is required by the load. There are two basic types of inverter that could produce the form of switching that is required. The switching produced by the series inverter occurs due to inductor and capacitor components forming an underdamped system. This produces a zero in current at some time during the conduction cycle and thus these circuits are often used in combination with Silicon Controlled Rectifiers (SCR). Part of the specification of this design requires the inverter to support the mains in powering a load. This in turn requires that the circuit has the ability to lock into the mains frequency. The series inverter is incapable of fulfilling this requirement since it cannot be commutated externally. The second type of inverter, the parallel inverter, is externally commutated.

The parallel inverter has many advantages over the series inverter. The parallel inverter is more efficient and also produces a square output voltage waveform. The parallel inverter has switches that can be turned on when desired. This method of switching produces a square wave as long as the switches S1 and S2 are driven by a square wave control signals, one control signal being exactly out of phase from the other by 180 degrees. Figure 1.1 shows the basic parallel inverter.

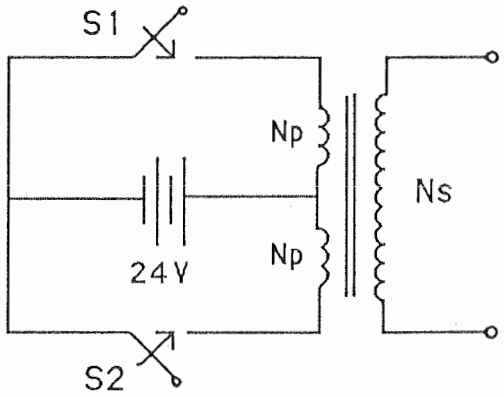

Figure 1.1: Parallel Inverter.

The square wave voltage on the secondary is the primary voltage multiplied by the turns ratio. This square voltage waveform is to be converted to a sinusoidal waveform by the use of an output filter.

1.2 Basic Inverter Requirements.

The inverter circuit was required to have two major modes of operation,

1.) To power a load independently of Mains power.
2.) To assist the Mains to power a load.

The inverter has three main components, a battery, a centre tapped transformer and two power transistors. The battery may consist of two 12 Volt batteries connected in series to form a 24 Volt battery or a single 12 Volt battery. Any batteries used would be previously charged from the solar cell or a combination of solar cells. It is recommended that the inverter be operated with the maximum battery voltage of 24 Volts since this produces the most

efficient circuit. The saturation voltage loss, or Vce sat, across the power transistors produces the major efficiency loss in the inverter. If a Vce sat of 1.5 Volts is assumed then this represents a loss of 6.25 % if the total battery voltage is 24 Volts. This loss would double to 12.5 % if the 12 Volt battery is used.

The inverter circuit was designed to produce a power of 500 Watts so the centre tapped transformer needed to be capable of handling about 500 VA. The turns ratio of the transformer had to be such that about 240 Volts rms were produced at the output of the filter. The power transistors chosen for the inverter were Motorola MJ 802's (NPN) which have a maximum collector current of 30 Amps and a power handling capacity of 200 Watts. Switching effects may produce large spikes across the primary windings so diodes were placed across the transistors to give them some protection.

CHAPTER TWO:

Transformer Design.

2.1 An Introduction to the Transformer Design.

The initial part of the design to be considered was that design of the transformer for the inverter. The transformer used last year, on this same project, was underpowered so it was recommended that a new transformer be designed and constructed. It was also recommended that the transformer have a toroidal core since this type of core has a low value of leakage reactance. The specifications for the transformer are the following.

1.) A Power rating of 500 VA.
2.) To have a centre tapped primary winding.
3.) That a voltage of at least 240 V_{rms} is achieved across the load after the filter.

Initially calculations were performed to find the most efficient transformer design and an idea of the most suitable size for the toroidal core. The maximum efficiency occurs when the core losses equal the copper losses. After this investigation was completed a Silicon-Iron core of suitable size was found.

2.2 Transformer Design Calculations.

The operation of the parallel inverter shown in Figure 1.1 was considered. A square waveform is produced on the primary winding by the use of transistors which switch the D.C. source across the primary winding. The D.C. source consisted of two 12 V batteries in series. The square wave voltage across the primary windings was 24 V amplitude.

The attenuation factors that need to be considered to determine the turns ratio are:

1.) The transformer losses.
2.) The filter losses due to the filter inductances having finite values of Q.
3.) The loss of regulation due to the leakage reactance of the transformer.

To overcome these effects it was decided that the peak value of the fundamental of the secondary would be made equal to 365 V. This gave a rms value of about 260 V. The peak value of the fundamental of the secondary square waveform would be,

$$= 24 * (n{:}1) * \frac{4}{\pi}$$

where, (n:1) = turns ratio.
4/pi = fourier coefficient.

The turns ratio was determined to be 1:12.

Since only the fundamental of the secondary square waveform is accepted by the filter all other harmonics are suppressed. These harmonics are also suppressed in the primary due to reflection in the transformer. Faraday's Law was then used to determine the number of primary turns,

$$N_p = \frac{E}{4.44\,\hat{B}A_c f} = \frac{24 * \frac{4}{pi} * \sqrt{0.5}}{4.44 * \sqrt{2} * 2.475 * 10^{-3} * 50} = 28 \text{ turns.}$$

and hence the number of secondary turns, N_S, was determined as 336 turns. The diameter of the both windings were found by considering power and current densities. The transformer was initially assumed to have an efficiency of about 95%, with losses in the filter contributing 1% loss overall. Therefore this part of the design assumed an overall efficiency of 94%. The actual power loss could now calculated since an output power of 500 W was required. The total power required was (500/0.95) or 532 W, so the total losses were 32 W with 25.6 W of power lost in the transformer. The power out of the transformer secondary was (532 - 25.6) or 506.4 W. Therefore,

$$I_S = \frac{506}{\frac{365}{\sqrt{2}}} = 1.96 \text{ Amps.}$$

and,

$$I_P = \frac{532}{\left(\frac{24 * \frac{4}{p}}{\sqrt{2}}\right)} = 24.6 \text{ Amps.}$$

The diameter of the windings were chosen as,

Primary B&S No.8, d_p= 3.26 mm.
Secondary B&S No.17, d_p= 1.15 mm.

Checking the current densities in the windings,

$$J_p = \frac{I_p}{A_p} = \frac{24.6}{\pi\left(\frac{3.26}{2}\right)^2} = 2.94 \text{ A/mm}^2$$

$$J_S = \frac{I_S}{A_S} = \frac{1.96}{\pi\left(\frac{1.15}{2}\right)^2} = 1.89 \text{ A/mm}^2$$

These values of current density are well below the value of 5 A/mm^2 so the windings were capable of withstanding the full load currents.

2.3 Transformer Tests.

After checking the design carefully, the core was wound and the normal short and open circuit transformer tests were conducted. The short circuit test gave the practical value of winding resistance to be 4.8 Ohms, in comparison, to the theoretical value of 3.7 Ohms. The difference between these two figures is due to the difficulty in winding the primary since the winding is 3.2 mm diameter and thus cannot be wound as tightly as a wire with smaller diameter. The theoretical calculation assumed that that the winding was wound perfectly. A leakage reactance of 1.85 mH was calculated. An efficiency of about 91% was determined from measurements. A value of regulation was calculated, using the formula derived in Appendix A,

$$r = \frac{1 - E_f}{2 E_f}$$

where E_f = Efficiency of the transformer.
The calculated value of regulation was 5%.

CHAPTER THREE:

Other Inverter Components.

3.1 Inverter Transistors.

A decision had to be made on the type of switching element that would be used in the inverter. The decision to use transistors over SCR's in this design was made since the transistor is more easily turned, both on and off. The fine frequency control that is a vital part of this design cannot be delivered by the SCR so transistors were used. The frequency control requirement can be met, by the use of transistors, since their operation is simply controlled by application of drive to their bases. This drive must be continuously applied during the of time that the transistor is required to be on.

The type of power transistors to be used had to be decided upon. These two transistors are responsible for producing a square voltage on the primary from the battery. Since the required frequency for switching is 50 Hz, then the transistor turn on time is negligible. The transistors were chosen so that their maximum collector current was able to cope with the 25 Amps flowing through the primary side of the circuit. The transistors chosen (MJ802) have a maximum collector current of 30 Amps and a power rating of 240 Watts. The power losses in the transistors can be calculated using the equation,

$$P_{loss} = V_{ce(sat)} * I_{c(max)} * \text{Duty Cycle.}$$

The duty cycle, for this case, is 1/2 since each transistors is only turned on for half the switching cycle. Assuming a $V_{ce(sat)}$ of 1.8 Volts and a $I_{c(max)}$ of 25 Amps, the power loss per transistor is 22.5 Watts. The total loss in the power transistors should be about 45 Watts.

3.2 Feedback Diodes.

Switching effects in the inverter circuit are capable of producing large spikes of voltage across the primary windings. Assume that one of the transistors has been turned on for a time and the signal from the drive transistors has just changed level. The base drive of the transistor will go to zero forcing the collector current quickly to zero. This rapid change in collector current produces a large voltage spike equal to L* di/dt across the primary windings. This spike was found to be large, about five times the battery voltage. Reflection of the spike occurs through the transformer, producing a very large voltage peak across the secondary winding. Hopefully a substantial portion of this spike can be prevented by the use of feedback diodes connected across the power transistors. A channel is provided, by using these diodes, for some of the high L*di/dt current components. This should help to provide a voltage waveform across the output of the transformer that is truly square.

Prevention of the voltage across either primary winding rising above the battery voltage is also achieved by use of these feedback diodes.

The diodes chosen for this role were:

Motorola MR754
High current lead mounted silicon rectifier.

3.3 Inverter Circuit.

The two feedback diodes and power transistors were mounted on two heatsinks. The transformer, the battery, the power transistors and the feedback diodes were connected in the layout shown below. Suitably sized fuses were connected on both the primary and secondary sides of the transformer.

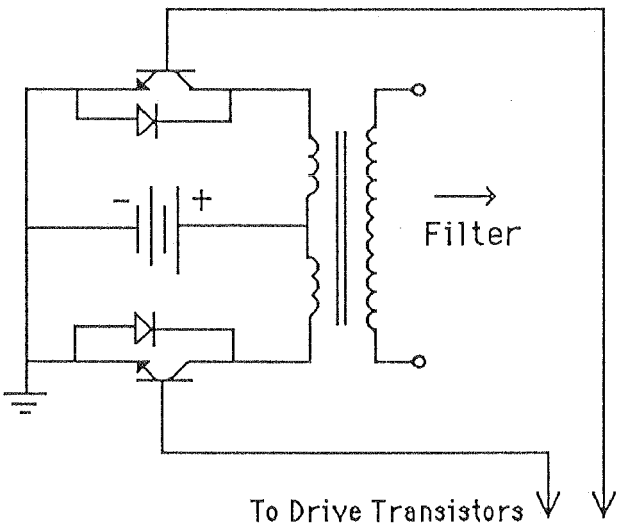

Figure 3.1: Complete Parallel Inverter.

CHAPTER FOUR:

The Output Filter.

4.1 Required Characteristics.

The filter's role in the circuit is to convert the square voltage waveform, produced at the secondary of the transformer, into a sinusoidal waveform that meets the required standards, to make it equivalent to 240 Volt mains supply. The filter is required to produce this output as well as incurring only minimal power loss. Therefore the filter has to be constructed from reactive components, capacitors and inductors. The inductors must be constructed so that their windings have minimal resistance associated with them.

The final requirement for the filter is that it's output is independent of the load. The filter must function within the stipulated guide-lines for both modes of operation.

4.2 The Basic Filter.

The standard form of the filter is the following:

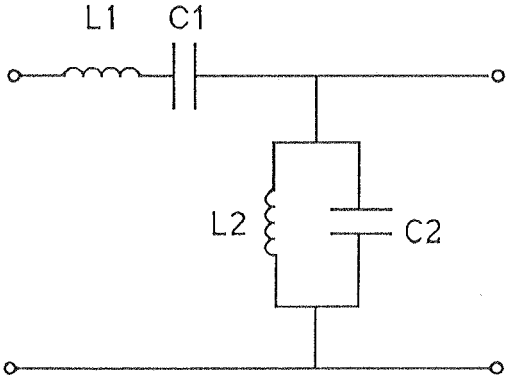

Figure 4.1: Basic Filter.

This filter is constructed from two tuned circuits, L1 and C1 forming a series resonant circuit and L2 and C2 forming a parallel resonant circuit.

$$Z_{in} = sL + \frac{1}{sC} = \frac{1 + s^2LC}{sC}$$

$$\text{If } S^2 = -\frac{1}{LC} \quad \text{then } w_r = \frac{1}{\sqrt{LC}}$$

The series resonant circuit appears as a short circuit at the resonant frequency. The filter's parallel resonant circuit appears as an open circuit at the resonant frequency. If the inductors in the filter are modelled practically, with small resistances in series with each inductance, then the filter should look like a small series resistance at the resonant frequency of 50 Hz. This filter was used for the independent mode of operation.

4.3 Mains Supporting Filter.

A small addition to the filter was required so that it was function correctly for the mode of operation supporting the mains. An extra inductor was added to the basic filter.

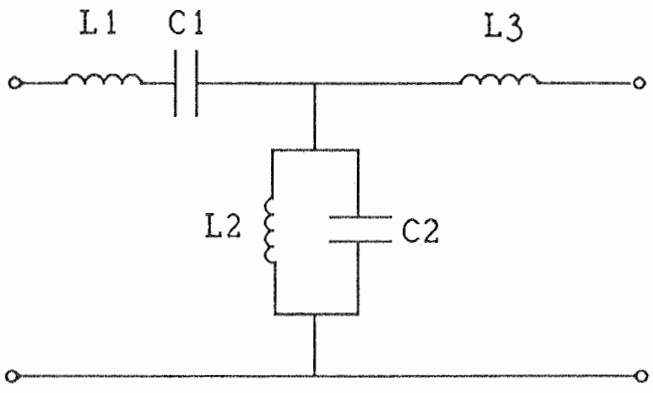

Figure 4.2: Filter for mains case.

The addition of third inductor allows the flow of power into the load to be controlled as in an alternator. This allows the phase of the output from the filter to be varied with respect to the mains. This in turn controls the effective power factor and the flow of power. The principles of phase control will be considered in greater detail later.

4.4 Final Filter Values.

The major analysis of the two filter combinations was performed (by my partner, John Kan) using a software called SPICE. The final component values derived from the spice analysis were,

L_1 = 0.90 H.
L2 = 0.50 H.
C_1 = 11.26 uF.
C2 = 20.56 uF.

The extra inductor for the mains case was determined as,

L3 = 0.377 H.

5.5 Capacitor Selection.

The final components required for the completion of the filter were the capacitors. A combination of capacitors had to be chosen that firstly gave a capacitance very close to the required value, and secondly was capable of withstanding the large voltages present on the secondary side of the circuit. The series capacitor (11.27 uF) would have a voltage in the order of 600 Volts rms or 850 Volts amplitude across it under full load conditions. The capacitor in the parallel resonant circuit would have about 240 Volts across it under similar conditions.

A decision was made to try and create the required capacitance values with capacitors that were readily available, to avoid the cost and delay of ordering. Initially an attempt was made to use greencap capacitors, but unfortunately the capacitance values were too low. The greencap capacitors had a voltage rating of 250 Volts D.C., so three of them had to be connected in series to obtain the correct voltage rating. The resulting capacitance becomes a third of the initial capacitance value if all three capacitors have the same value.

Some large oil and paper capacitors were obtained. These capacitors were 'large', both in their physical size and capacitance value. The largest of them also had D.C. voltage ratings of 415 Volts. Combinations of these capacitors and greencaps were connected together in trial and error fashion in an attempt to achieve the correct capacitances, while still maintaining the required voltage rating. The final combinations of the capacitors are shown below. The value shown in the brackets are their respective D.C. voltage ratings.

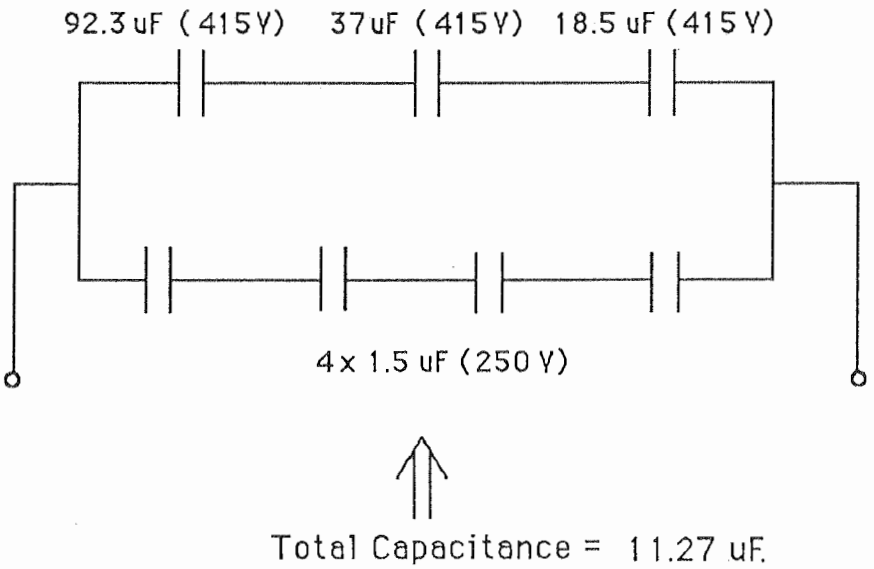

Figure 4.3: 11.27 uF Capacitance.

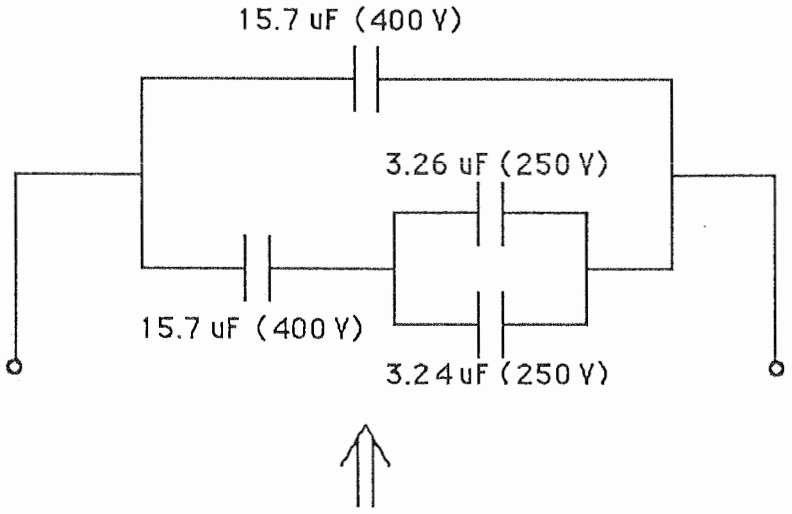

Figure 4.4: 20.3 uF Capacitance.

CHAPTER FIVE:

Inductor Design.

5.1 Requirements for the Inductors.

The next stage of the project involved the design and construction of the inductors required for the filter. Since the values of current on the secondary side of the circuit are quite high (around 2 Amps) then the inductors need to be designed by the use of windings around a Silicon-Iron C-core. To fulfil the requirements of the filter design the Q factors of these inductors must be around 100. The values of the inductors required are 0.9 H, 0.5 H and 0.377 H. Since the Q factors, the inductance values and the amount of current passing through the inductors is high, a substantial cross-sectional area of core is required.

Initially a number of E-cores and a large C-core were found. Calculations predicted that the core with the largest cross-sectional area (the C-core) was unable to achieve the required Q value. The high value of current forces the airgap between the cores to be increased so that the iron does not go heavily into saturation. This high value of airgap combined with the large value of inductance makes the number of required turns to be high. Since there is only a finite amount of space for the windings to be wound around the core, a large number of turns forces the diameter of the windings to be small, which in turn creates a larger resistance. Increasing this value of resistance decreases the Q value of the inductor. Thus difficulty arose in achieving the required value of Q.

A core with a larger cross-sectional area was required. A larger E-core was found and calculations indicated that this core would be acceptable for the 0.9 H inductance. Although a large number of turns were again required the larger core enabled the

diameter of the windings to be increased, thus keeping the resistance of the windings and the Q factor to an acceptable value.

These effects make the physical size of the inductor reasonably large but it must be remembered that they are being used in a power application. The values of inductance were found to be able to be varied by plus or minus two percent with the output of the filter still keeping within the Australian Standards for harmonic distortion.

5.2 Former and Winding Arrangement.

The calculations for the design of the inductors would have been simpler if only C-cores had been used. The C-cores that were readily available were not of sufficient size however, so E-cores had to be used. Both of the cores were wound so that a maximum window area was available for the windings. This allowed the largest diameter of wire to be used since the inductance value in this case was proportional to the square of the number of turns. For the case of the E-cores the window area available for windings was maximised by using two windings, each being wound around the outside legs of the E-cores. The figure 5.1 shows this.

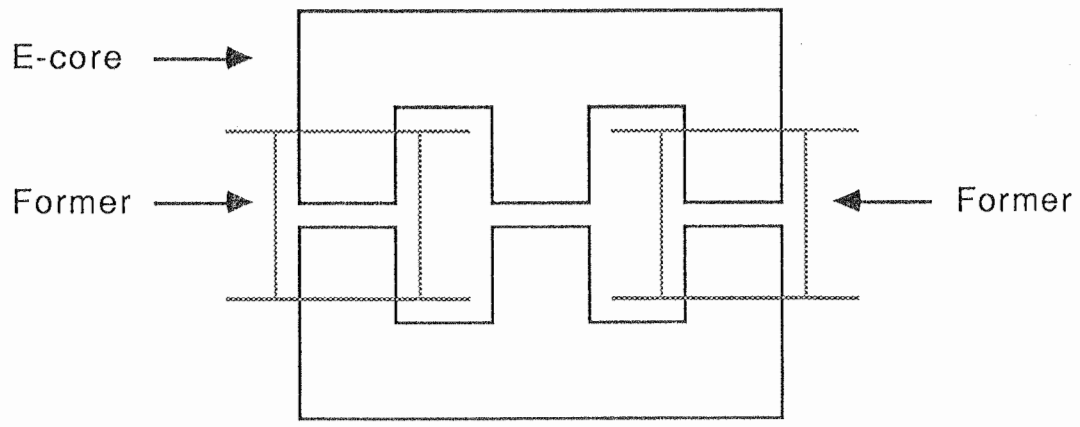

Figure 5.1: E-Core Former Arrangement.

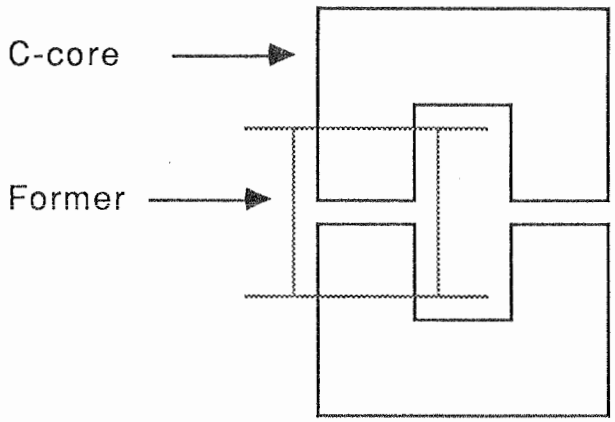

Figure 5.2: C-Core Former Arrangement.

Therefore two formers were required for each inductance constructed from an E-core. One former was required for the C-core.

The presence of two formers on the E-core now presented a problem. Since there were two separate windings there were two possible ways the windings could be connected. The windings could either be connected in series or in opposition. The figures 5.3 and 5.4 show the different winding arrangements.

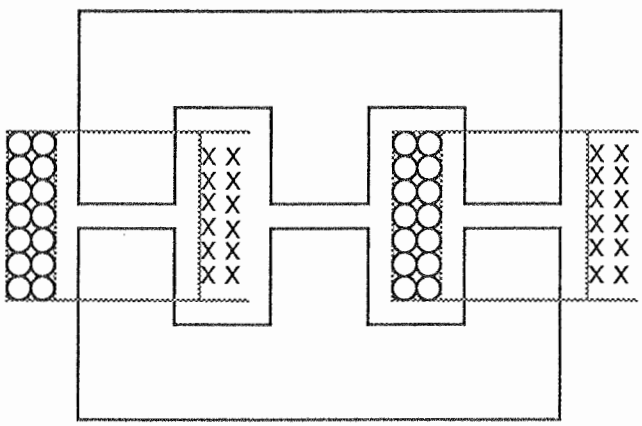

x Winding goes into the page.
O Winding comes out of the page.

Figure 5.3: Winding Arrangement A.

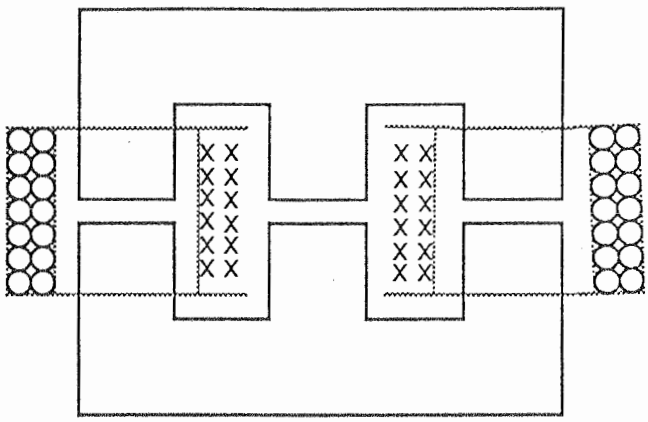

x Winding goes into the page.
O Winding comes out of the page.

Figure 5.4: Winding Arrangement B.

An investigation had to be made to find out which winding method produced the highest value of inductance. A test was first conducted to verify the relationship between inductance and the number of turns with a coiled reactor.

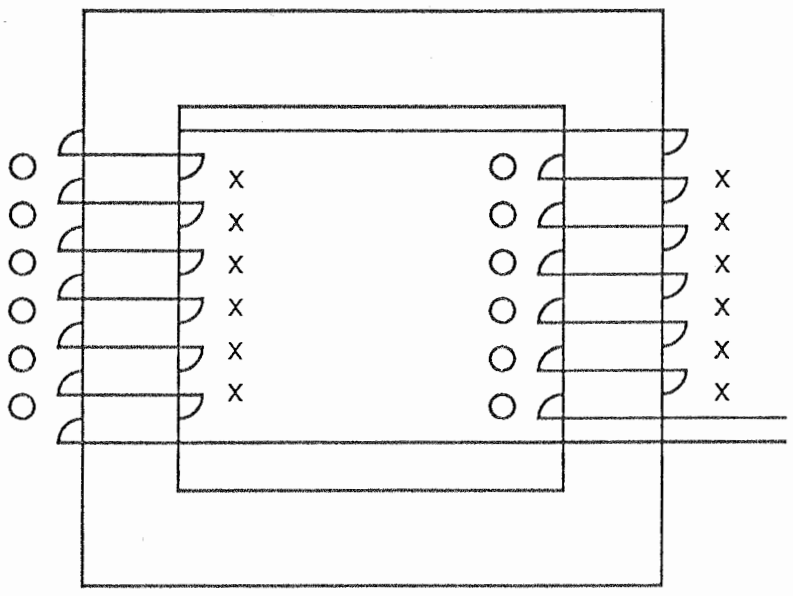

Figure 5.5: Coiled Reactor Winding Arrangement A.

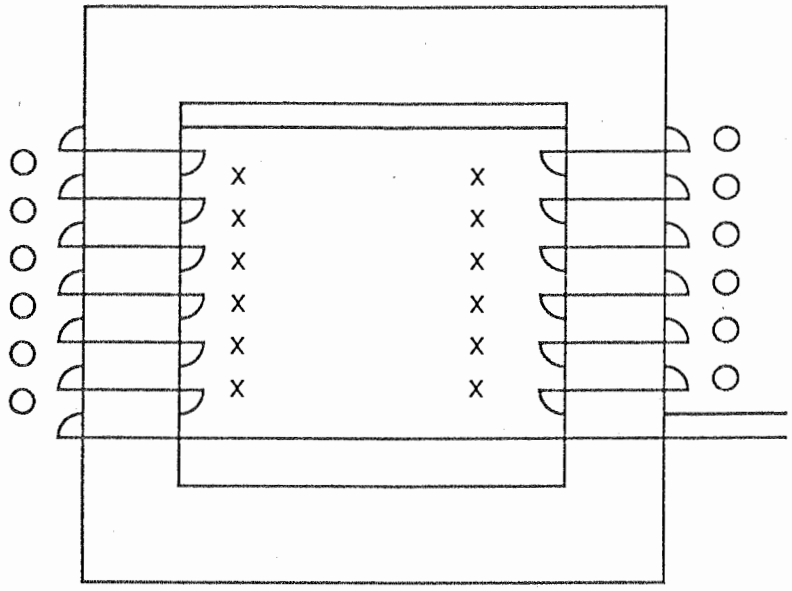

Key: x Windings going into the page.
O Windings coming out of the page.

Figure 5.5: Coiled Reactor Winding Arrangement B.

In Case A, the two windings are effectively in series so the ampere-turns produced by passing a current through the windings should add. In Case B the windings are opposing so the ampere-turns should subtract. If the number of turns on each of the windings of Case B are the same then the ampere-turns should totally cancel. The effective magnetomotive force (m.m.f.) and flux in the core should be zero due to the equation:

$$\text{Flux} = \frac{\text{Magnetomotive Force}}{\text{Reluctance}}$$

Since the inductance of the circuit is proportional to the flux passing through the core, the inductance of Case B should theoretically be zero.

Firstly the impedance of one single winding (assume that this winding has N turns) was measured and found to be about 6 Ohms. Two windings were then connected as shown by Case B. The impedance of this circuit (which now has 2N turns) was found to be about 24 Ohms.

The effect of the resistance of the windings can be ignored due to their large diameter so the measured impedances are effectively reactances. Since the inductance of the core is given by,

$$L = \frac{N^2 A_c u_o}{2.0g}$$

the inductance is proportional to the square of the number of turns. Therefore the expectation would be that the reactance of Case B would be 4 times that of the single winding case, since it has twice the number of turns. The reactance values obtained verify this ratio.

The connection between the windings was then reversed as in Case A. An impedance of 1 ohm was measured which suggests that the majority of the ampere-turns, were cancelling. These tests also confirmed the thought that maximum inductance would be produced if the windings were wound so that the ampere-turns added (as in Case B.).

5.3 Preliminary Inductor Testing.

A decision was made to perform preliminary tests to find the accuracy of the inductor design equations. It was hoped that any effects of leakage flux and other inaccuracies could be measured and then compensated for in the final design of the inductors.

Initially a test was performed on a C-core. A number of turns were loosely wound around the core. An A.C. voltage source was connected across the 'inductor' and the current and voltage was measured so that the circuits impedance could be calculated.

The theoretical value of the inductors reactance was calculated by the use of the equation,

$$X_L = \frac{2\pi f u_o A_c}{2.0\, g} = wL$$

where, N = number of turns.
m_o = permeability of free space.
A_c = effective cross-sectional area of the C-core.
g = effective airgap (twice the gap between the cores).

The derivation of the inductance equation (from which the reactance equation was derived.) is shown in Appendix B. The resistance of the windings was found by meter measurement to be 0.4 ohms. Impedance measurements were conducted for two different airgaps one being 1.54 mm and the other 5.08 mm. The following results were obtained.

Table 5.1: Preliminary Test Results.

g (mm)	$Z_{measured}$ (ohms)	$R_{measured}$ (ohms)	$X_{measured}$ (ohms)	X_{theo} (ohms)	% Difference
1.54	1.15	0.40	1.08	0.96	10
5.08	0.57	0.40	0.41	0.23	70

These results seem to be quite inaccurate when compared with the theoretical calculations, especially in regard to the percentage difference between the measured and theoretical reactances for the 5.08 mm airgap case. One encouraging sign from these results was that the measured reactance values (and related inductance, X_L = wL) were found to be larger than theoretical calculations predicted. The increase in the value of inductance most probably occurred due to the presence of leakage

and fringing flux.. It is possible that the inductance equation could be altered to include these effects i.e.,

$$L = \frac{N^2 u_o A_c k}{2.0\,g}$$

where the leakage and fringing effects are equal to the factor k, which would be equal to some positive value. Although these effects are certainly helpful in terms of achieving a certain value of inductance, the careful designer cannot use them to lower the amount of turns (and hence increase the value of Q) since the amount of inductance produced by leakage and fringing flux is hard to predict.

Similar tests were performed on several E-cores, with variations in quantities such as E-core size, airgap and number of turns. Varying this number of parameters gave a large amount of data enabling verification of the E-core inductance equations. These equations are derived in Appendix B. Some difficulty was found winding the cores by hand since no formers were used. In some cases the sharp corners of the cores penetrated through the enamel insulation on the copper wire causing short circuits. This problem was recognised after very inconsistent results were obtained. Existence of this problem was simply checked by seeing if there was infinite resistance between the ends of the windings and the cores, by use of an electric multimeter.

After the results were examined it was found that the inductances calculated from measurements were greater than those calculated from the theoretical equations. The occurrence of this inconsistency was again assumed to be due to the effects of leakage and fringing flux. The actual design of the inductors could now begin, knowing that the measured inductance would exceed

the value predicted from the theoretical equation. The inductance could then be lowered to the required level by gradually reducing the number of turns and measuring impedance levels in a trial and error fashion.

5.4 Inductor Design Example.

The method used to design the 0.9 Henry inductance will be used as a design example. The E-core chosen for this inductance had a effective cross sectional area of 1452 mm^2. This area is the area at the bottom of one of the legs. An airgap, g of 3.0 mm was used. Rearranging the inductance equation,

$$L = \frac{N^2 u_o A_c}{2.0\ g} \quad \text{gives}$$

$$N = \left(\frac{2.0\ L\ g}{A_c u_o}\right)^{\frac{1}{2}} = 1720 \text{ turns}$$

Now the magnetic field strength can be calculated,

$$B_{rms} = \frac{N u_o I}{2.0\ g} = 0.72\ T$$

This value must be lower than 1 Tesla so that magnetic saturation of the core does not occur. If significant saturation occurs then the inductance of the magnetic circuit will be proportional to the amount of current passing through it. The design requires inductors whose inductance values are independent of the current flowing through them.

MMF = NI = 3440 Ampere turns.

The area available for the windings to be wound for this E-core is 6720 mm^2. Assuming a current density J, of 0.76 A/mm^2 and a spacing factor of 0.7 then the area required for the windings can be calculated.

$$\text{Area} = \frac{NI}{J \ S.F.} = 6450\,mm^2$$

The required number of windings will be able to fit in the available window space. Now,

$$\text{Area of conductor, } A = \frac{I}{J} = 2.5\ mm^2$$

which gives the diameter of the windings, d to be 1.83 mm. This diameter of copper wire corresponds to B & S No. 13.

An estimation of the Q factor of the inductor can now be made. The E-core was measured and the mean length of turn, L_t was estimated to be 332 mm.

$$L_t = L_{mt} * N = 571\ m.$$

The resistance of the winding can be found knowing the resistivity of copper, r equals 2.0 * 10^{-8} Ohm-metres.

$$R = \frac{r\ L_t}{A} = 4.6\ \text{Ohms}$$

The copper loss in the winding equals $I^2 R$ or 18.3 Watts. The magnetisation loss for the E-core was found to be 6.0 Watts so the total loss is 24.3 Watts. The A.C. resistance of the circuit is $(24.3/2^{2)}$ or 6.1 Ohms. Therefore,

$$Q = \frac{2.0\pi f L}{R_{ac}} = 46.6$$

An identical technique was used to design the other two inductors. The figures calculated for each of the inductors are shown in Table 5.2.

Table 5.2: Inductor Values.

Inductance (H)	Type of core	Airgap (mm)	Turns	Theoretical Q
0.90	E-core	3.0	1720	46.6
0.50	C-core	1.0	772	49.3
0.38	E-core	2.4	1550	24.0

The 0.90 H and 0.5 H inductors can be seen to have a theoretical Q factors of about 45 and 50 respectively. These values were accepted. The design of the 0.377 H inductance on the other hand was found to only have a Q factor of 24. Initially this value was deemed unacceptable and an attempt was made to it.

5.5 Two Core Inductor Investigation.

It was thought that if two separate cores were used in the construction of this inductor then the effective window area would become larger, enabling the diameter of the windings to be increased, decreasing it's overall resistance. It was found that the situation was not helped by the use of this method. The problem with this method is that the number of turns of the inductor is proportional to the square root of the inductance value. To explain this effect an example will be considered.

Assume an inductance of 3H is required and is going to be designed by using 2 cores, one inductance being of value 2H and the other of value 1H.

Table 5.3: Relationship between No. of Turns and Inductance.

Inductance (H)	Number of turns = k * $\sqrt{\text{inductance}}$
3	$k(3)^{0.5} = k*1.73$
2	$k(2)^{0.5} = k*1.41$
1	$k(1)^{0.5} = k*1.00$

If one core is used the number of turns equals k.1.73 where k is a constant of proportionality (For k to be truly constant the values of airgap and core cross-sectional area must not change between the one core and two core cases). If two cores are used the total number of turns would now equal k*1.41 plus k*1.00 or k*2.41. Therefore the number of turns required using two cores is greater than if only one core is used. Increasing the number of turns decreases the value of Q. The are three main effects in designing the inductor with two cores instead of one.

1.) The effective window area is increased.
2.) The cross-sectional area of iron is increased.
3.) The required number of turns is increased.

The first two effects enable the Q factor of the inductor to be increased but the third has the opposite effect. The combination of the three effects only marginally increased the value of Q in our case. It was then decided that using two cores for the 0.377 H inductance was not beneficial considering the extra time and materials that would be used. The marginally lower value of Q that was achieved by using the single core was considered acceptable.

The values of Q, shown on the Table 5.2, are lower than the value of 100 that was initially specified for the filter but these design values are the best that could be managed with available materials. Drawings of the formers required for each of the cores were completed allowing them to be constructed out of bakelite.

5.6 Inductor Testing.

All three inductors were then constructed and tested. The inductance values measured were found to be greater than the values predicted from the theoretical equations. These results were in line with the conclusions from the earlier testing. Fine tuning of the inductance values was now required so that their values were within at least two percent of the initial design values. There are two possible ways of lowering the inductance values, either increase the dimension of the airgap or decrease the number of turns. The second method was used since its effects were more gradual, as long as only a relatively small number of turns were taken off between measurements. The final values for each of the inductors were the following:

Table 5.4: Final Inductor Values.

Required Inductance (H)	Designed Number of turns	Actual Inductance (H)	No. of turns removed	% of turns removed
0.90	1720	1.073	165	9.6
0.50	772	0.573	43	5.6
0.377	1550	0.480	158	10.2

Required Inductance (H)	D.C. resistance of winding (ohms)	Final Inductance (H)	% diff. from designed inductance	Estimated Q
0.90	3.2	0.906	0.67	60.5
0.50	1.6	0.494	1.20	65.0
0.377	5.1	0.379	0.53	31.5

These figures show that between 6 and 10 percent of the number of turns calculated in the original design had to be taken off the cores before the correct values of inductance were measured. The final inductance values shown in Table 5.4 were measured under full load current conditions. As the current was gradually increased to full load variations in the impedance of the circuits were observed. Since the inductance values are to some degree dependent on current, it would be expected that the filter performance may vary depending on the current. The testing of the filter may show some deviation in filters characteristic with changing load current indicating that some degree of magnetic saturation is present in the inductor cores.

The difference between the designed and final inductance values was well within the allowable two percent deviation. The last column of figures of Table 5.4 show new estimations for the Q values for each of the inductors. The new estimations were calculated after the D.C. resistances of the inductors were measured thus enabling improved estimates of the value of the copper loss. The initial design estimates of D.C. resistance were high in comparison to the measured figures so the initial estimate of the Q factor were low. The magnetic losses in the circuits were unabled to be measured so the theoretical figures calculated in the design were assumed to be correct.

Finally, the voltage waveform across the inductors was displayed on a Cathode Ray Oscilloscope, to see whether there was any distortion on the waveform. Distortion effects will occur if there exists a significant degree of magnetic saturation in the core. The distortion checks were performed with full load current flowing through the inductors, since the degree of magnetic saturation will be highest in this case. No effects of distortion could be seen so it was assumed that the effects of magnetic saturation were minimal.

All the figures for the inductors constructed from E-cores (i.e. 0.90 H and 0.377 H) are with the two windings connected in an arrangement to give the maximum inductance. Additional measurements were recorded, for both these inductors, with the windings connected the opposite way which results in a lower value of inductance. This result actually has little relevance to the overall design, but is interesting, especially in seeing if all the E-core inductance derivations are correct. These derivations are shown in Appendix B. A sample of the results taken are shown below. The first table shows the results for the 0.90 H inductor core with the windings connected to give the maximum amount of inductance.

Table 5.5: Inductance Comparisons.

Applied Voltage (Volts)	Current (Amps)	Impedance (Ohms)	Reactance (Ohms)	Inductance (H)
121.4	0.4	302.8	302.8	0.96
178.4	0.6	294.3	294.3	0.94
232.0	0.8	290.0	290.0	0.92
290.0	1.0	288.0	288.0	0.91

The following results were obtained with the windings, on the E-core, reversed.

Applied Voltage (Volts)	Current (Amps)	Reactance (Ohms)	Inductance (Henries)	Ratio
52.6	0.4	131.5	0.42	2.3
77.8	0.6	129.7	0.41	2.3
102.8	0.8	128.5	0.41	2.2
127.6	1.0	127.6	0.41	2.2

The final column of numbers, in Table 5.5, shows the ratio between the inductances of the different E-core winding arrangements. The derivation predicted that this ratio should be 3:1 not the 2.2 to 2.3:1 ratio actually measured. The deviation of this ratio away from the theoretical result most probably occurred due to the different winding arrangements creating different fringing and leakage flux patterns. An identical set of results were taken for the 0.377 H inductor and the ratio between the two cases was again found to be 2.2 to 2.3. The practical results seem quite consistent which suggests that the actual size of the E-core does not effect the proportion of fringing and leakage flux to flux in the iron.

CHAPTER SIX:

Phase Control.

6.1 Phase Control Operation.

This section will describe the application of phase control to the design. In the Mains supportive mode of operation the inverter circuitry can be simplified to the following form. The series resonant circuit becomes a short circuit at 50 Hz, while the parallel resonant circuit is effectively an open circuit. This leaves the third inductor, and its series resistance, across both the inverter's sinusoid voltage waveform and the mains supply.

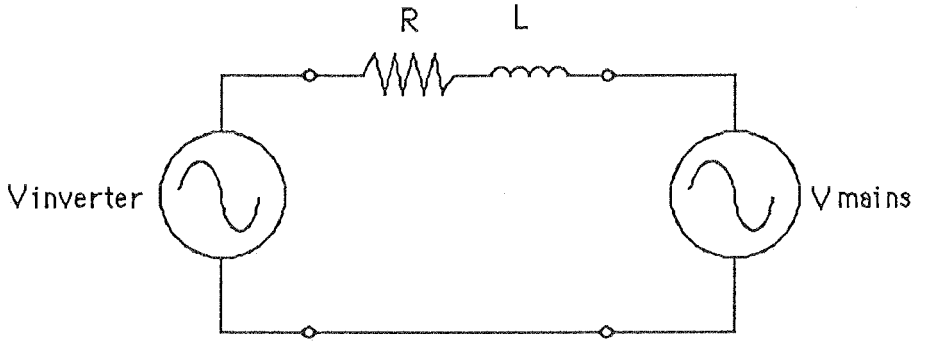

Figure 6.1: Equivalent Circuit.

The Phase control circuitry is involved in controlling the difference between the phase of the inverter in relation to the phase of the mains. Varying amounts of power flow occur from altering the phase difference from 0 to 180 degrees. The circuit has the following phasor diagram,

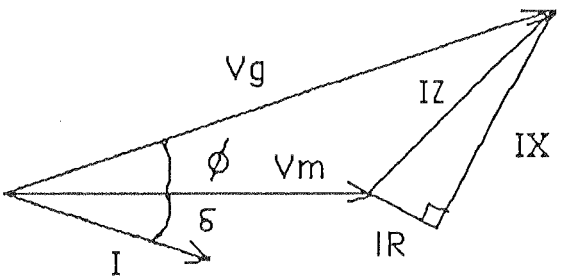

Figure 6.2: Phasor Diagram of Mains Case.

where, Vg = Voltage generated by the inverter.
Vm = Mains Voltage.

The frequencies of the two voltages must be the same but their amplitudes need not be the same. The voltage Vg must lead Vm. Robert Ivory derived the equation that describes the flow of power in his thesis.

$$\text{Power} = \frac{V_m(V_g * \text{Cos}(d - \emptyset) - V_m * \text{Cos}(d))}{Z}$$

, where d= delta.

In our case the resistance of the inductor is much less than the reactance of the inductor so the resistance can be ignored. Thus the power equation can be simplified into the following form,

$$\text{Power} = \frac{V_m * V_g * \sin(\emptyset)}{Z}$$

The angle theta represents the angle of the phase difference between the inverters voltage and the mains. If theta is made to equal zero then no power will flow. If the angle becomes equal to 90 degrees then maximum power will flow. An angle of 180 degrees again results in no power flowing. It can be be concluded that the phase control circuitry will need to be capable of varying the phase between 0 and 90 degrees.

6.2 Phase Control Circuitry.

Initially the phase control circuitry designed by Robert Ivory was built and tested to see if this met our requirements. Parts of the circuit were redesigned. A diagram showing the circuit layout is shown in Figure 6.2.

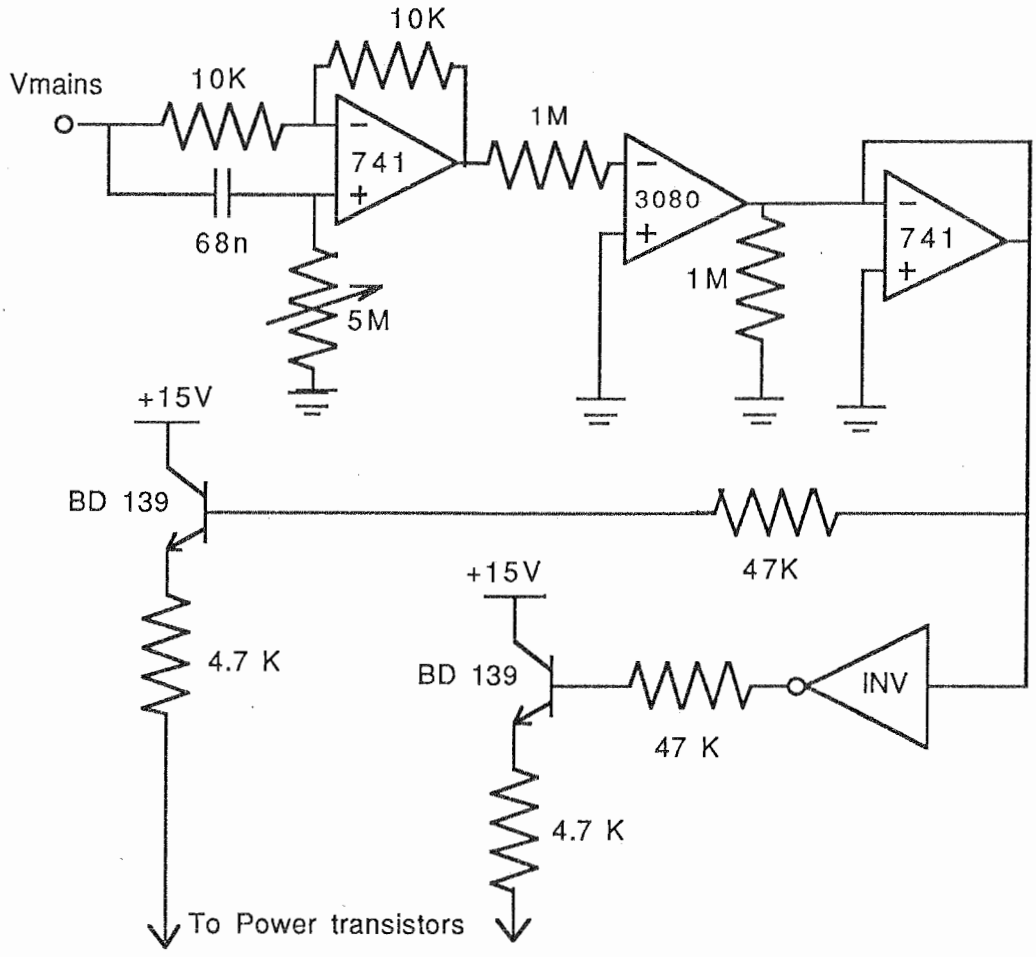

Figure 6.2: Phase Control Circuitry.

The whole basis of the control of power, for the mains supportive mode of operation, is dependent on controlling the phase of the output of the inverter in relation to the phase of the mains supply. It is the role of the phase control circuitry to produce this control over the phase of these two voltages.

The control circuitry shown above can divided into three main sections,

1.) Phase Circuit.
2.) Zero Crossing Detector.
3.) Drive Circuit.

Firstly consider the Phase Circuit. After analysis of the operational amplifier was completed the transfer function of the circuit was found to be,

$$\frac{V_{out}}{V_{in}} = \frac{sRC - 1}{sRC + 1}$$

Thus the phase circuit is effectively an all-pass filter. The phase of the output can be controlled, in respect to the mains supply, by adjusting the 5 MOhm potentiometer.

The zero crossing detector determines when the output of the phase circuit goes through zero. The output of the Z.C.D. is a square wave, which cuts through zero at the same time as the output from the phase circuit, but is 180 degrees out of phase in respect to it. The major role of the Z.C.D. is to produce a square wave suitable for switching purposes.

A buffer circuit is placed after the zero crossing detector to enable the other two sections of the circuit to be isolated from the rest of the inverter. This buffer had a high input impedance and a low output impedance.

The output of the buffer is connected to two points, one point feeds directly to a BD139 drive transistor. The other, passes through an inverter, and then feeds the second drive transistor. This process enables complimentary square waves to be generated, which are required for switching. The resistance values were chosen so that the necessary amount of drive could be provided to the power transistors.

The phase control circuitry was built and tested. Photographs of the output of the mains controlled oscillator are below, the first showing the oscillator square wave being 180

degrees out of phase with the mains (i.e. No power flow). The oscillator is 90 degrees out of phase with the mains (i.e. the condition under which maximum power flows) in photograph 2.

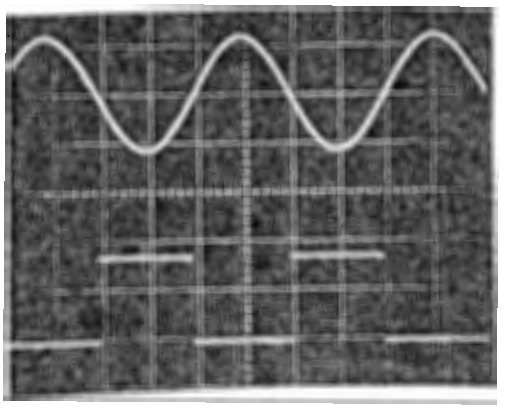

Photograph 1.

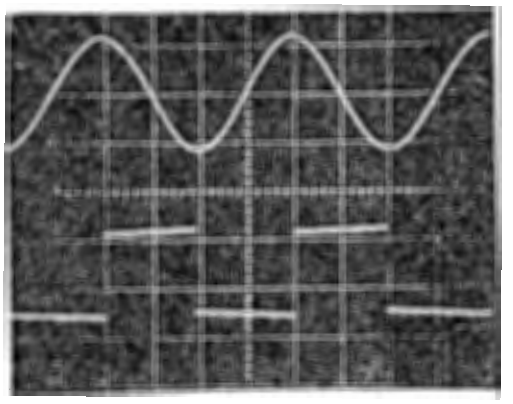

Photograph 2.

Photograph 1 shows the mains controlled oscillator, 180 degrees out of phase with the mains supply.

Photograph 2 shows the mains controlled oscillator, 90 degrees out of phase with the mains.

CHAPTER SEVEN:

Powering a Load Independent of the Mains.

7.1 50 Hz. Oscillator.

Now the mode of operation will be considered where power has to be supplied to a load independent of mains power. A 50 Hz oscillation must be produced so that the transistors are turned on and off at the required frequency. A number of possible solutions have been considered to this problem:

1.) Three inverters connected with an RC network.
2.) A crystal producing a clock that can be logically divided to give the required 50 Hz.
3.) Voltage controlled oscillator.

The third case was disregarded as its principle operation is to produce an oscillation whose frequency is dependent on an adjustable voltage. Since our system requires a fixed frequency of oscillation, variation of the frequency is not required.

The first idea of using three inverters connected with an RC network was then investigated. The oscillator was built and the values used for the capacitance were varied to gain an oscillation close to 50 Hz. One initial problem with this circuit was that the square wave output did not have a one to one mark-space ratio. After trying several different chips (each chip contains six inverters) this problem was improved. After testing, the resistance was replaced with a combination of two potentiometers so that the oscillators frequency could be varied with ease. One of the potentiometers was used for coarse frequency control, while the other enabled fine tuning. The frequency of the generated oscillation could now be made almost exactly 50 Hz.

The oscillator circuit that was designed is shown below.

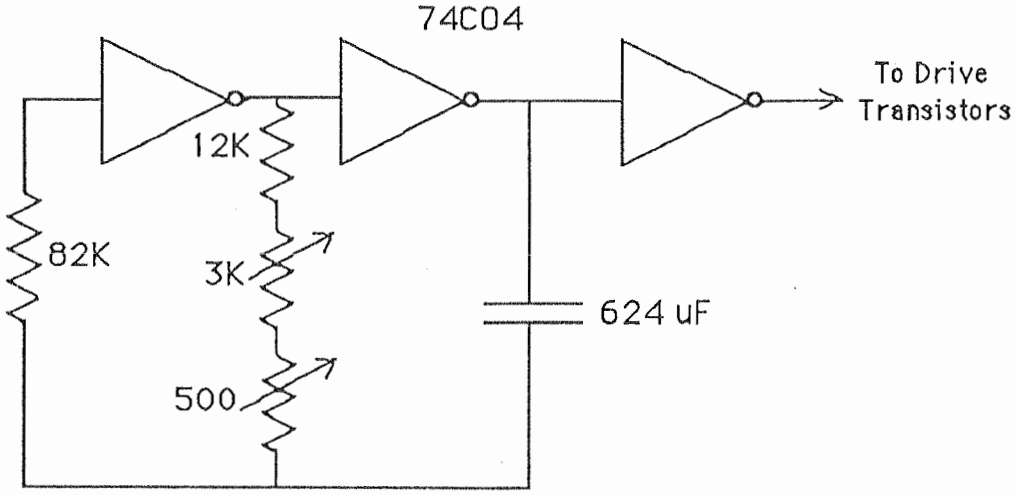

Figure 7.1: 50 Hz. Oscillator.

The full inverter circuit for both modes of operation can be displayed.

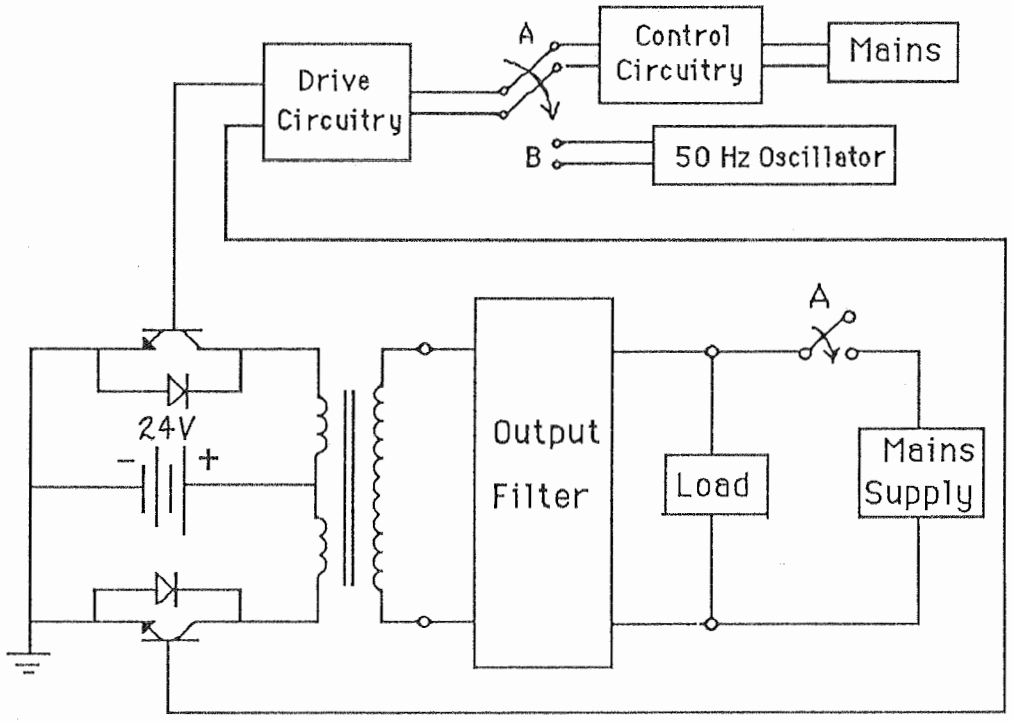

Case A: Mains Assisting Mode.
Case B: Independent Mode.

Figure 7.2: Inverter.

7.2 Testing of the Inverter using passive load.

After the construction of the final inductor, the filter was completed, and thus we were in a position where some significant testing of the inverter could be conducted.

The independent mode control circuitry was used to produce the required square wave signals that were fed into the drive transistors. The square waveforms produced by the drive circuitry was continuously monitored by the use of a C.R.O. A photograph of the complementary switching waves are shown below.

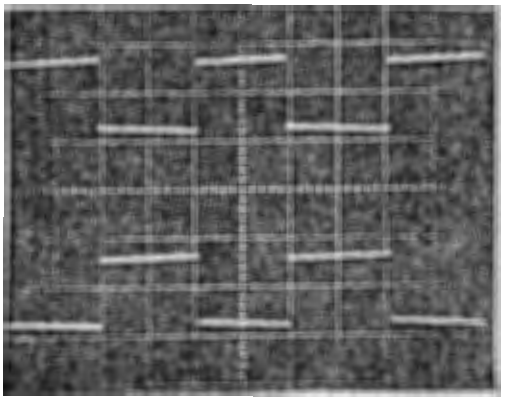

Photograph 3.

Photograph 3 exhibits the complementary switching waves.

The inverter was initially tested with a 12 Volt D.C. source instead of the full battery voltage of 24 Volts. A large resistance was used as the load, so the inverter was only lightly loaded. The combination of the low D.C. source and the large resistive load resulted in only a low power being generated.

The output voltage of the filter was found to be of sinusoidal form. A distortion meter enabled the overall distortion of the waveform to be determined as 3% of the fundamental. The distortion produced from the mains supply was then found to be about 2%. Although, at this time, the distortion of the inverters output was greater than that produced from the mains, the value of distortion from the inverter fell well within the standards set for primary and secondary distribution. An A.C. power analyser was then used to measure the individual harmonic components as well as frequency, power, voltage and current values. Photographs 6 and 7 (Page 49) show the sinusoidal output voltage for different power levels.

The load resistance was then lowered enabling the level of power in the load to rise. The resistive load, to give the required power, in the load was previously calculated to be,

$$R_{F.L.} = \frac{\text{Output Voltage}}{\text{Full Load Current}} = \frac{240.0}{1.96} = 120 \text{ Ohms}$$

Numerous quantities were observed and measured while the power was increased. These quantities included,

1.) Output Power in load.
2.) Output Voltage.
3.) Current through load.
4.) Supply Current flowing from the D.C. supply.
5.) Frequency.
6.) Frequency Harmonics.

A number of irregularities were noticed as the output power was increased, the most noticeable being the D.C. supply whose voltage lowered dramatically as more current was demanded. Another irregularity observed, including a large drop in output

voltage as the load was decreased. At this point in time, it was unknown whether these effects, at the output, were primarily caused by the drop in D.C. voltage at the supply.

This drop in voltage at the terminals of the D.C. supply can be explained easily. The actual batteries that supply this voltage are connected by long lengths of conductor, from the basement of the Engineering building to the D.C. Plugboard in the Power Lab. The inverter required large currents from the supply (about 15 Amps), at high power level. This large current produced a substantial voltage drop along the length of the conductors.

This voltage drop was clearly effecting the results from the inverter, so a decision was made to acquire some D.C. Batteries. Two 12 Volt batteries were used for the rest of the testing (each about 30 Amp-hours). A single 12 Volt battery was used initially, to operate the inverter at a lower power. The D.C. supply was then increased to the specified value of 24 Volts.

A test, similar in nature to that conducted previously, was performed with the power in the load being slowly increased while various quantities were monitored. The voltage being produced from the battery was found to be of a steady magnitude while the output power was fluctuated. The following irregularities were observed.

1.) The maximum output power peaked at a value of about 200 Watts not the designed value of 500 Watts.

2.) A decrease in load voltage was observed as the power in the load was increased.

3.) The square waveform produced over the primary windings was seen to distort the distortion becoming worse at higher powers.

4.) The amount of harmonic distortion in the output voltage waveform was seen to increase.

Each of these circuit characteristics need to be considered, so reasons for their existence can be deducted and possible solutions to the problems formulated. It is also very important to consider whether any of the irregularities are interrelated.

7.3 Maximum Output Power.

The maximum power dissipated at the output was measured as 200 Watts. The inverter circuit was designed to handle powers up to 500 Watts, so the circuit is either having difficulties in producing the power, or some components of the circuit are dissipating much more power than expected. The low value of power observed is the result of a drop in output voltage, so this power problem is closely related to the regulation problem.

The lack of power at the output may be caused by the following reasons,

1.) The transformer being unable to deliver the required power.
2.) A breakdown in the control switching square wave.
3.) Unexpectedly large power losses occurring in the power transistors, the transformer or the filter.

7.4 Regulation Difficulties.

A lowering of the output voltage was observed as power produced by the inverter was increased. The regulation difficulty became more extreme at maximum power. The graph, below of output voltage vs. power shows the drop in output voltage at high power.

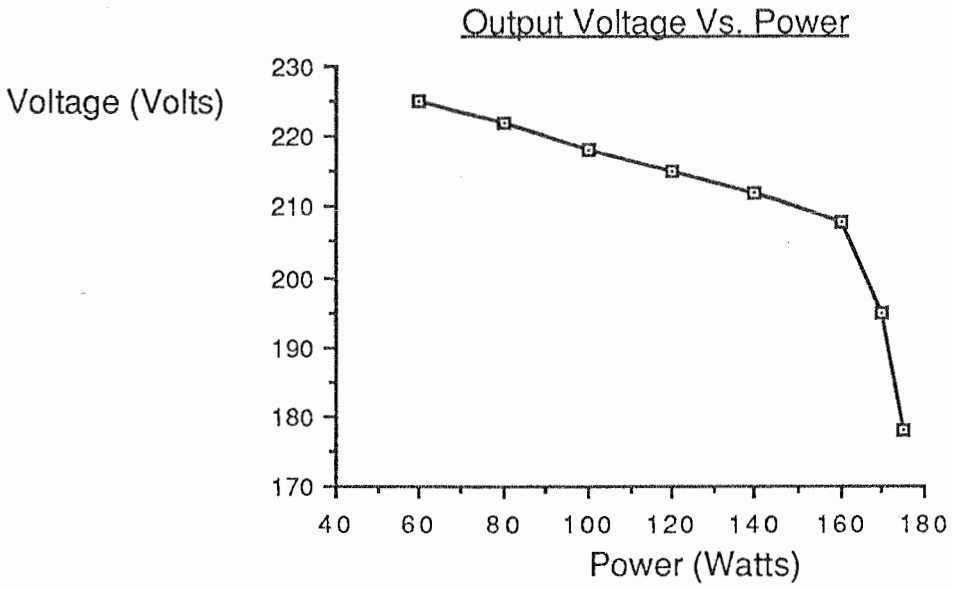

Graph 7.1: Output Voltage Vs. Power.

The regulation, assuming 180 Watts as being a full load value, was found to be about 26 %. Attempts were made to find the source of the large voltage drops that were responsible for the poor regulation. The transformer and/or the filter inductors were suspected. A test was conducted to find the power and regulation that the basic inverter circuitry could provide without the filter connected. The resistive load was placed directly across the secondary of the transformer. The load was decreased steadily, until a power of 250 Watts was dissipated. The inverter circuit was incapable of producing any power in addition to this.

Graph 7.2 displays the Voltage produced at the secondary of the transformer (without the filter).

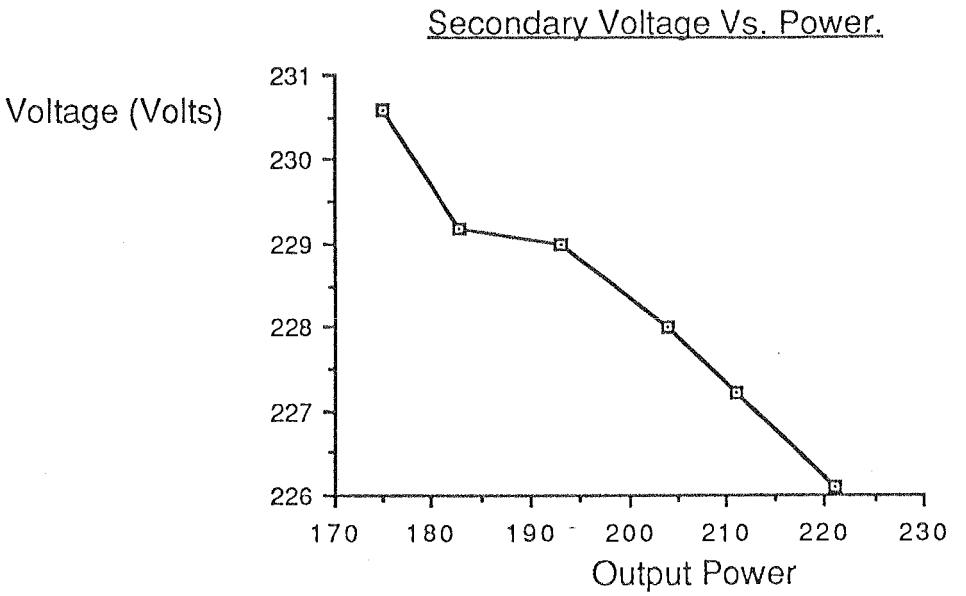

Graph 7.2: Transformer Secondary Voltage Vs. Power.

The no-load voltage was measured as 244.0 Volts so the regulation of this part of the circuit was calculated as 7.3 %, using 220 as a full load value. This regulation figure seems reasonable for this part of the circuit. The results of the test indicate that the regulation problem most probably occurred due to losses in the inductors. Photographs were taken of this stage of the circuit, under no load and full load conditions. Improvement in the switching of the inverter can be seen at higher powers.

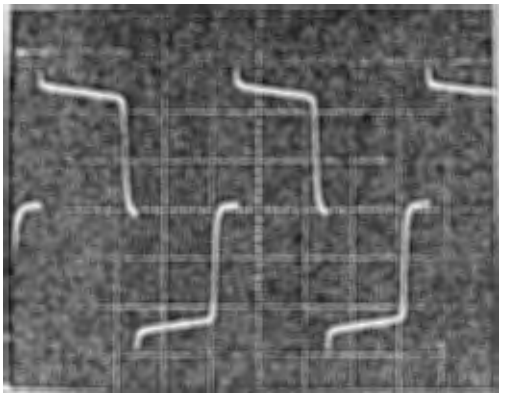

Photograph 4.

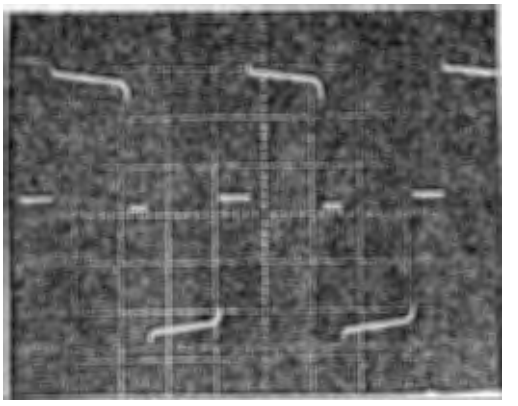

Photograph 5.

Photograph 4 shows the output of the secondary of the transformer under no load conditions. V_{rms} = 244.0 Volts.

Photograph 5 displays the output of the transformers secondary at a power of 250 Watts. V_{rms} = 220.0 Volts.

7.5 Breakdown of the Primary Voltage Square Wave.

At higher powers the waveforms produced across the primary windings distorted from the expected square waveform. The breakdown in the square waveform can be seen in the transition from photograph 6 to photograph 7. Photograph 6 displays the primary voltage at an output power of 160 Watts. The power had been increased to 180 Watts when photograph 7 was taken. Clearly a large voltage drop has occurred from the expected square wave level. The dips in the waveform indicate that the filter is presenting a sizeable impedance to the secondary of the transformer at 50 Hz. This suggests that the filter is not behaving as a true short circuit at that power level. The photograph also shows small areas of zero voltage, when the square wave is trying to switch between high and low voltages. These regions of the 'square' waveform, as well as the non-symmetrical nature of the distortion, indicate that some problem exists with the switching.

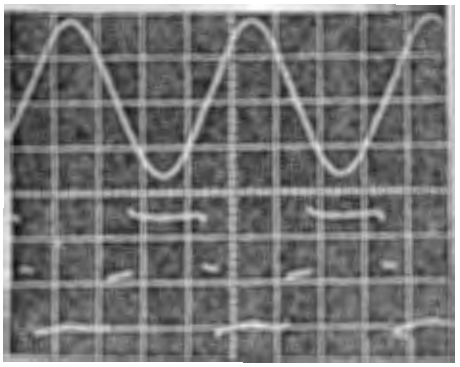

Photograph 6.

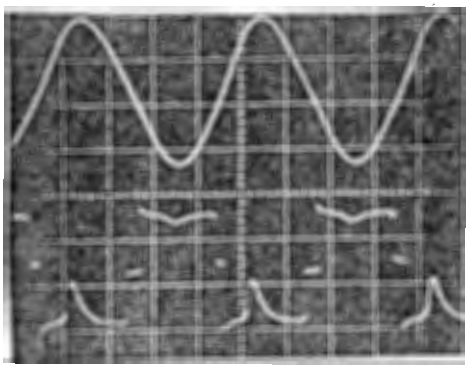

Photograph 7.

Photograph 6 shows the sinusoidal output from the filter, with respect to the voltage across the primary windings. The output was measured at 160 Watts, 50 Hz, V_{rms} = 187 Volts, Load current = 0.96 Amps and Harmonic Distortion = 2.48 %.

Photograph 7 displays the same quantities but with the output power at 180 Watts, 50 Hz, V_{rms} = 211 Volts, Load current = 0.77 Amps and Harmonic Distortion = 4.75 %.

7.6 General Discussion about Harmonic Distortion.

An increase in the total amount of harmonic distortion, as well as the individual harmonic components, was observed as the power was brought up. The increase in total harmonic distortion indicates that the filter is not performing as well as expected. Ideally the performance of the filter should be independent of the load. The predominant harmonics were found to be the second and third.

Some discussion of the relationship between the harmonics and the inverter circuit is required. The second harmonic of the waveform describes its symmetrical nature (i.e. are the positive parts of the circuit the same shape and magnitude of the negative parts?). The amount of second harmonic in the waveform is dependent on the performance of the switching circuitry, especially in regard to the mark space ratio of the switching square waves. The amount of third harmonic, and higher order odd harmonics, in the output is a measure of the filters ability to prevent the transmission of frequency components outside the passband, as well as the purity of the switching waveforms.

7.7 Switching Waveforms and the Second Harmonic.

Graph 7.3 displays the relationship between the percentage of second harmonic in the output voltage waveform and the output power.

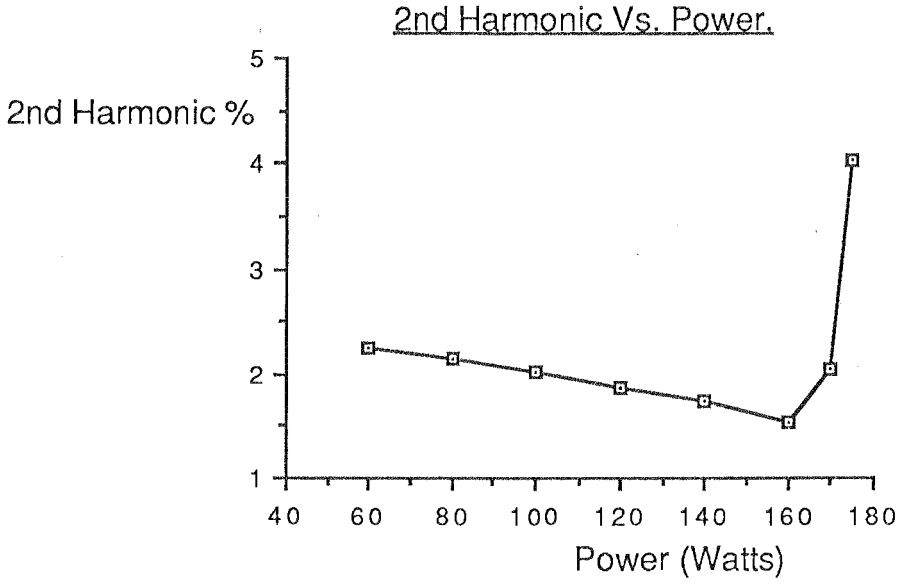

Graph 7.3: Percentage Second Harmonic Vs. Power.

Initially the magnitude of the second harmonic decreased, as the load was reduced, suggesting that the performance of the switching circuitry was improving. This improvement was probably due to the increased powers in the primary side of the circuit, switching the power transistors on harder. The difficulty that the switching circuitry had in producing a perfect square waveform under lightly loaded conditions can be seen on photograph 4. This effect may have been caused by dead zones in the power transistors. By the time the output current and power quantities had plateaued, the second harmonic component had risen sharply. The size of the second harmonic percentage suggested that the symmetrical nature of the switching waveforms had been lost. The end result of this occurrence was an unsymmetrical output waveform.

7.8 Filter Performance and Odd Harmonics.

The magnitude of the component of the third harmonic and other odd harmonics increased with increasing power.

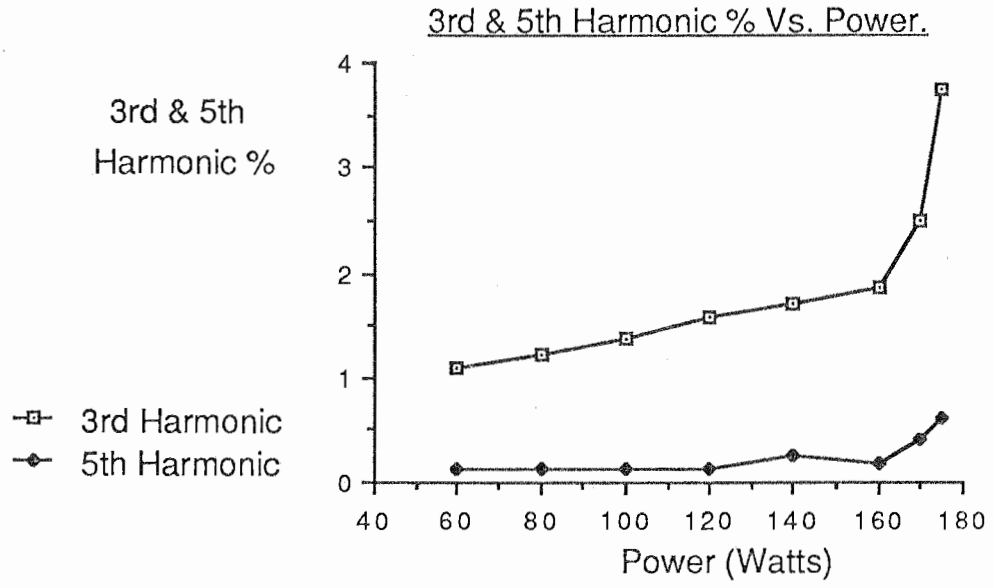

Graph 7.4: Percentage Third and Fifth Harmonic Vs. Power.

The increase in third harmonic indicates that the filter performance was degrading. The filters performance is primarily dependent on values of inductance and capacitance combined to form it. The changing value of third harmonic suggests that,

1.) The combination of the inductors and capacitances does not result in the filter having the required resonant frequency.

2.) The inductance values of the inductors are more dependent on the amount of current passing through them than was previously thought. If this is the case then the filter will have a resonant frequency that varies dependent on the current flowing through the filter.

More discussion is required on this last point. Some variation of inductance value with increasing current was noticed during the separate testing of each of the inductors. The inductors were 'tuned' by removing turns until their values were close to those required by the filter analysis. The inductors were 'tuned' so that the required inductance was produced while full load current was passing through them. Contrary to measurements, it would be expected that the third harmonic component would improve as the current through the filter was increased. Switching effects may be the cause of the problem.

7.9 Estimation of the Filter's Resonant Frequency.

Clearly some investigation was required to find the resonant frequency of the filter, as well as seeing if the resonant frequency was variable, depending on the load. An estimation of the resonant frequency of the filter was found by minimising the third harmonic component. The frequency of the passive load oscillator was varied by the use of an potentiometer. The second and third harmonic percentages were recorded and plotted on the graph below with the load power equal to 60 Watts.

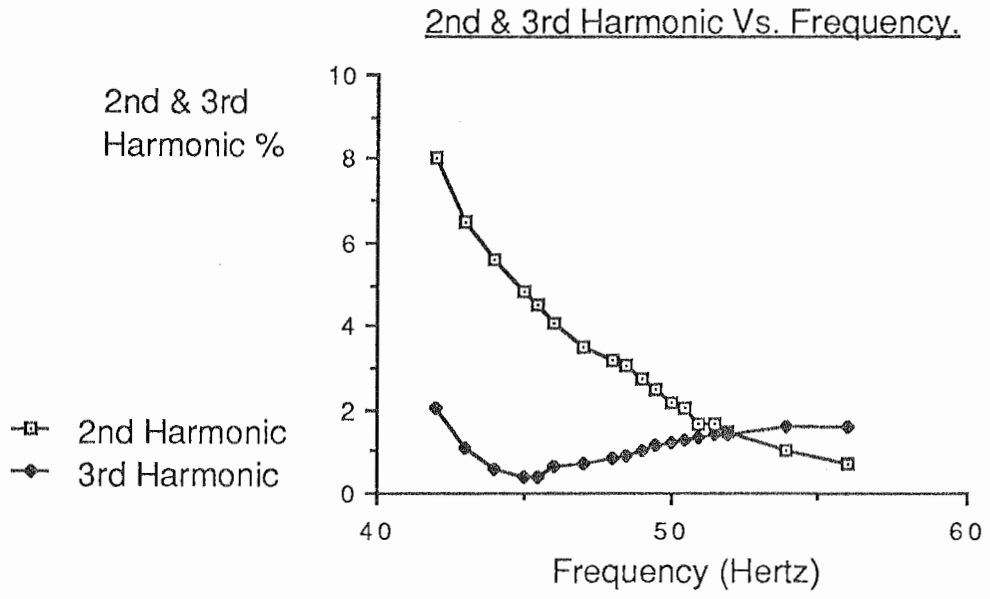

Graph 7.5: Percentage Second and Third Harmonic Vs. Frequency.

If the assumption is made that the resonant frequency occurs when the third harmonic percentage is lowest, then the resonant frequency of the filter at this power seems to be 45 Hz. The power level was then increased in steps, with the frequency being varied until the third harmonic was minimum. This frequency was recorded at each power level. The graph below shows the trend of increasing third harmonic with power.

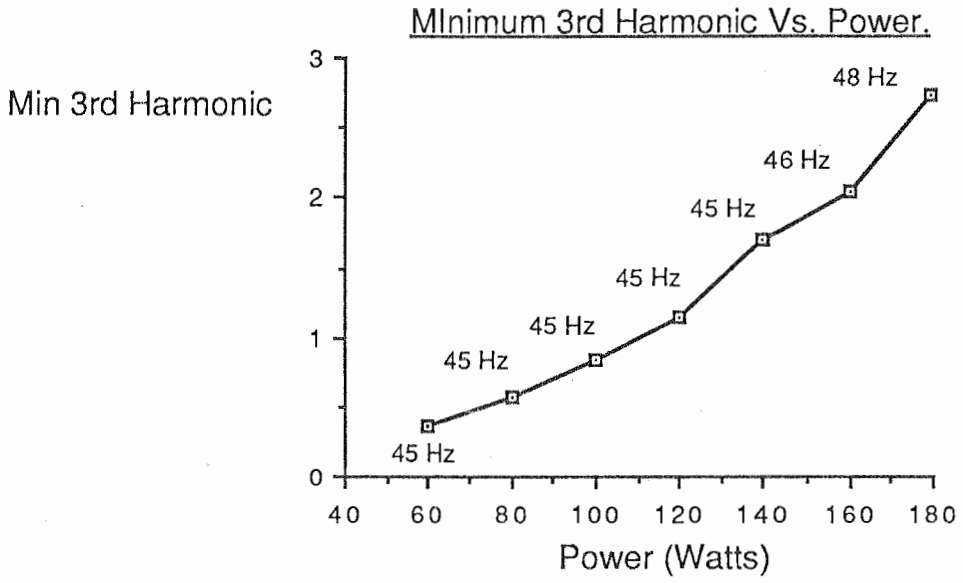

Graph 7.6: Minimum Percentage Third Harmonic Vs. Power.

The frequencies of the minimum third harmonics are shown beside their relative points. This frequency increased towards 50 Hz, until the power was restricted. These results may suggest that the filter is performing closer to specification at higher powers.

7.10 Efficiency Measurements.

The efficiency of the inverter circuit was also calculated by measuring the input and output powers. These measurements were recorded for low to high powers so that the range of efficiencies could be determined.

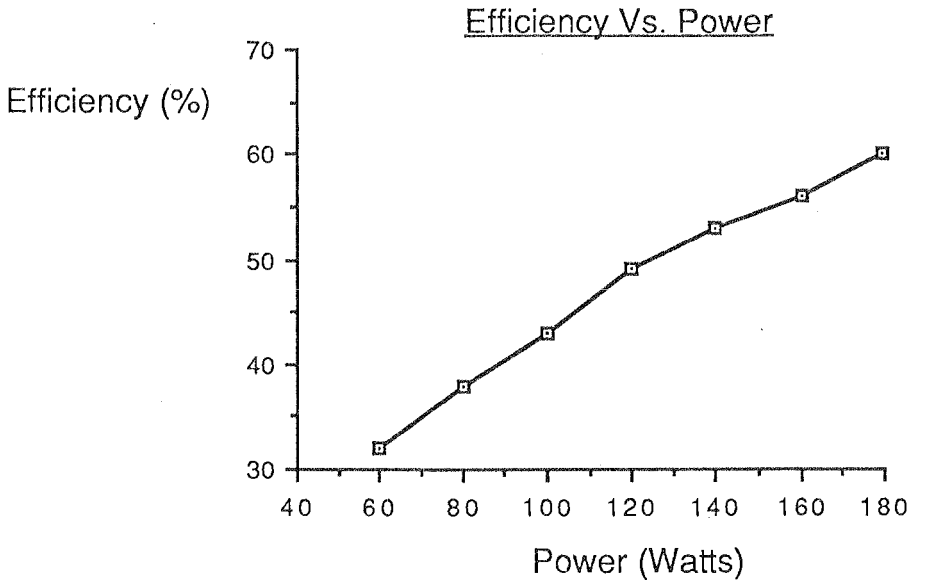

Graph 7.7: Efficiency Vs. Power.

The efficiency of the circuit can be seen to rise with increasing power. This result was expected since the losses occurring in the power transistors remain constant throughout. The proportion of the power loss in the power transistors to output power is less at higher powers. The highest efficiency measured from the inverter was about 60%. This figure seems low, but improvement will certainly be obtained if higher output powers can be generated.

7.11 Types of Passive Loads Tested.

At this point in time, the inverter circuit has been tested successfully with three types of load, these being,

1.) A Purely Resistive Load (i.e. test results already discussed.)
2.) A 60 Watt Light Bulb.
3.) A 375 Watt Power Drill.

The second and third loads were tested cautiously, with a rheostat being placed in series with them, to prevent any trouble that may be caused by large inrush currents. The power through the loads was then increased by lowering the resistance of the rheostat. The light bulb was brought up to maximum power while the drill was run up to a respectable speed.

CHAPTER EIGHT:

Conclusions.

8.1 Progress of the Design.

The recommendations made by Robert Ivory in his thesis, last year were the following:

1.) Design and building of a more suitable, higher powered transformer.
2.) Building of the output filter.
3.) Investigation into the self operating mode control circuitry.
4.) The design of an improved phase control circuitry.

All these recommendations have been investigated this year. The transformer, which was designed to have a power handling capacity of 500 VA, was built. The parallel inverter was built, incorporating the transformer with power transistors and feedback diodes mounted on heatsinks.

The output filter was re-designed, using the SPICE program, by my partner, John Kan. The filter's inductors were designed and constructed, while the required capacitances values were obtained.

The self operating mode control circuitry was devised using a 3-ring oscillator. This mode of operation was then tested, with the power being increased to 200 Watts.

The phase control circuitry was re-designed, and the required phase control was achieved. A trial of the mains supportive mode of operation was not conducted, due to the regulation problems at the output of the filter.

8.2 Further Investigations.

Although this design has progressed very well this year, with a large amount of work being completed, there still exists extensive scope for future investigations.

Initial investigations would need to be centred around the existing inverter circuit so that the irregularities observed could be overcome. Overcoming these problems would lead to the output power being increased to the original goal of 500 Watts, with corresponding improvements in efficiency and regulation.

Solving the regulation problem would enable testing of the mains supportive mode of operation. A form of feedback control could be developed for this operation mode. This would require monitoring of voltage and power levels.

The solar power side of this design has yet to investigated in any depth. The question has to be asked whether the batteries can be permanently connected to the solar cells, or will one set of batteries power the inverter while a back-up battery is charged by the solar cells. For the mode of operation, without the mains, there is a possibility that the D.C. power to the primary side of the transformer may be supplied directly from the solar cells. A high level of insolation would be required to power a light load. When insolation drops below the need of the consumer a back-up battery would be connected.

Finally a control system could be designed whereby the position of the solar cells could be altered to maximise the amount of sunlight that falls on them.

Appendix A:

Derivation of Transformer Regulation Equation.

The VA rating of a transformer is the Volts-Amps constant of both the primary and secondary windings. In practice, a transformer will always have an efficiency less than 100%. The power lost in the transformer is,

$$\text{Ploss} = \text{Input Power} - \text{Output Power}$$

$$= \frac{VA}{E_f} - VA$$

where Ef = Efficiency of the transformer. For greatest efficiency, half the losses of the transformer will be copper losses, and the other half will be iron losses in the core.

$$\text{Copper losses} = (I_{sec})^2 R = \frac{1}{2}.P_{loss}$$

By substitution and rearrangement,

$$R_{es} = \frac{V_{sec}}{I_{sec}}\left(\frac{1 - E_f}{2E_f}\right)$$

Let r, be equal to the regulation of the transformer's output at maximum current.

$$I_{sec}\ (R_{es} + jwL_{es}) = r.V_{sec}.$$

Thus,

$$L_{es} = \frac{V_{sec}}{I_{sec}\, w}\left(r^2 - \left(\frac{1 - E_f}{2E_f}\right)^2\right)^{1/2}$$

The relationship between the minimum regulation of a transformer and its efficiency is,

$$r > \left(\frac{1 - E_f}{2E_f}\right)$$

Appendix B:

Derivation of the Inductance Equations.

The inductance equations were derived by the use of an analogy which relates quantities in a magnetic circuit to quantities in an electrical circuit. Examples of this analogy are the following.

Magnetic Quantity:	Electrical Quantity:	
Flux	Current	
Magnetomotive Force	Electromotive Force	
Reluctance	Resistance	(etc.)

Firstly consider the case of a C-core.

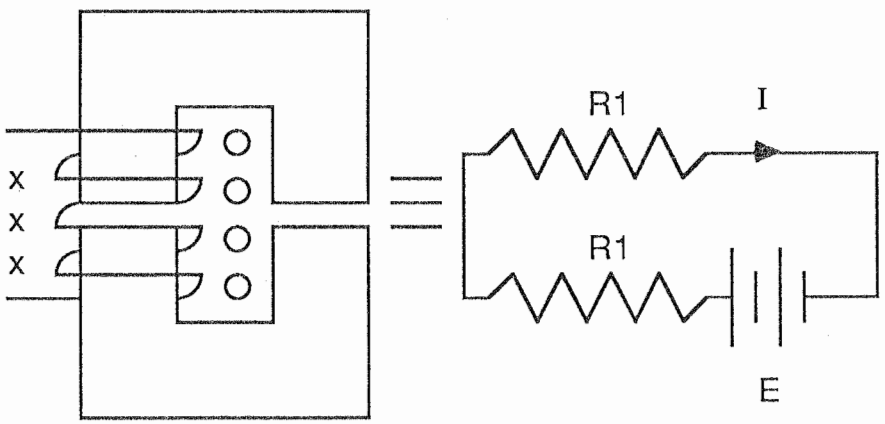

Figure B.1: C-core Analogy.

Each quantity of the magnetic circuit on the left can be related to a quantity involved with the related electrical circuit on the right. Each of the resistances R1 are equivalent to the reluctance values of each of the airgaps between the C-cores. The reluctance of the iron of the C-core is assumed to be negligible. The current, I, is equivalent to the flux flowing through the magnetic circuit. The electromotive force, E, is equivalent to the magnetomotive force produced from passing current through the winding. For this case we will assume that the winding has N

turns. Now the electrical equations describing the electrical circuit can be related to magnetic equations that will describe the magnetic circuit.

$$I = \frac{E}{2.0\,R_1} \quad \equiv \quad \emptyset = \frac{MMF}{2.0\,Rel} \qquad \text{where Rel = Reluctance}$$

Since,

$$Rel = \frac{g}{u_o A_c}\ , \quad MMF = NI \quad \text{and} \quad L = \frac{N\emptyset}{I}$$

then,

$$L = \frac{N^2 u_o A_c}{2.0\ g}$$

So the inductance of the C-core magnetic circuit above can be found using this equation. Now consider the case of the E-core wound with a single winding of N turns around the centre leg.

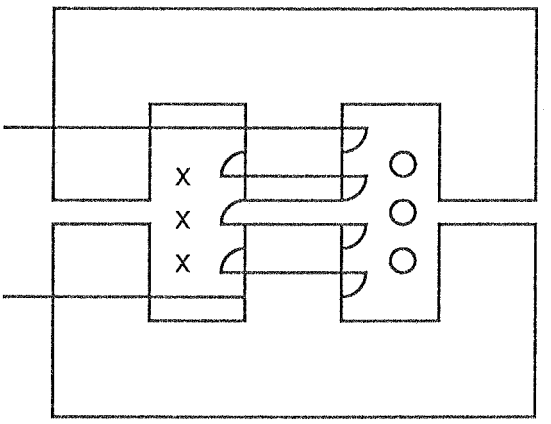

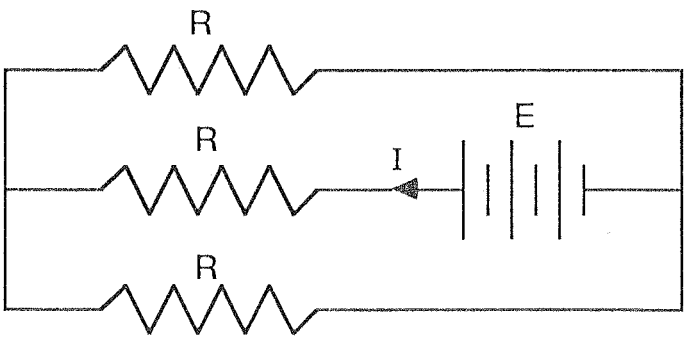

Figure B.2: Single winding E-core circuits.

$$I = \frac{E}{R_1 + 0.5\,R_1} \quad \equiv \quad \emptyset = \frac{MMF}{Rel + 0.5\,Rel} \qquad \text{where Rel = Reluctance}$$

Since,

$$Rel = \frac{g}{u_o A_c}\ , \quad MMF = NI \quad \text{and} \quad L = \frac{N\emptyset}{I}$$

then,

$$L = \frac{N^2 u_o A_c}{1.5\,g}$$

The two most important cases were considered next. These involve winding the E-core with a winding on each of the outer legs of the core. Each of these windings have N/2 turns on them (giving a total of N turns.). Consider the diagrams below.

Case 1.

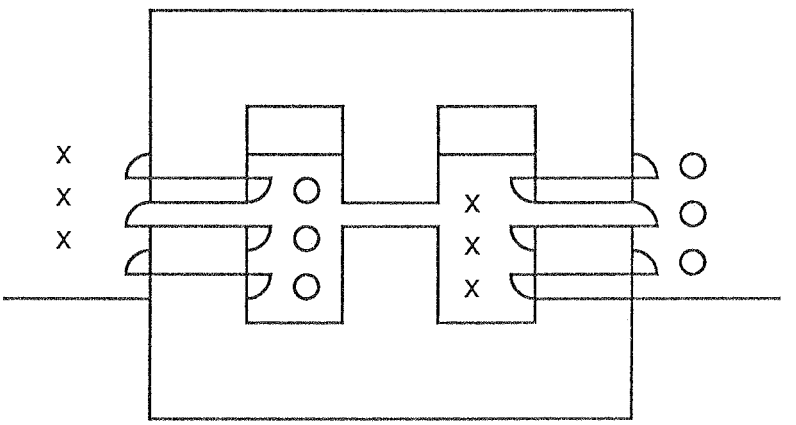

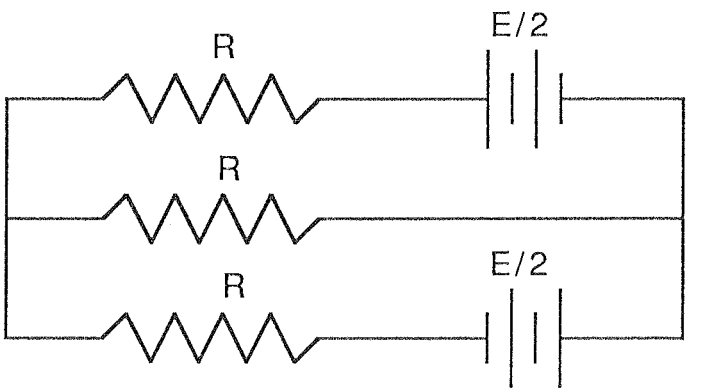

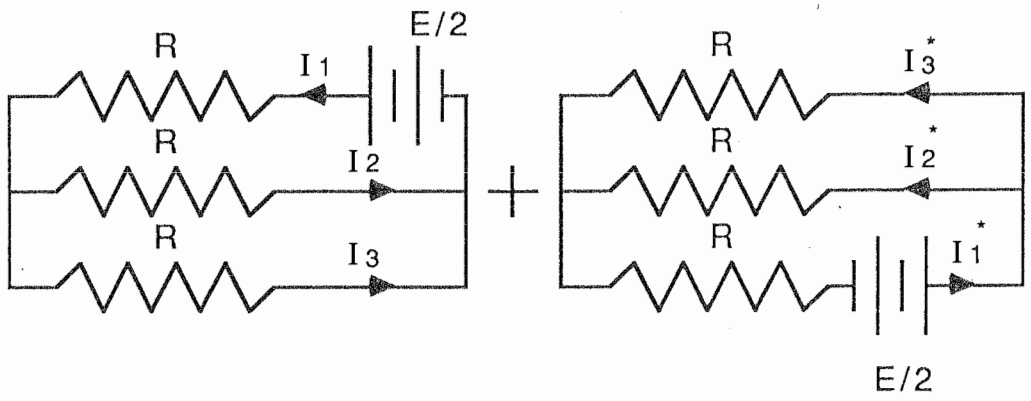

Figure B.3: Two Windings, Arrangement 1.

The electrical circuit equivalent has been split into two separate circuits by the use of the Superposition Theorem. The values used for the electromotive force are now E/2 Volts since half the number of turns on each leg of the E-core produces half the amount of magnetomotive force. Each of these circuits can now be analysised.

$$I_1 = I_1^* = \frac{0.5\,E}{R + 0.5R} \qquad I_2 = I_2^* = 0.5\left(\frac{0.5\,E}{R + 0.5R}\right)$$

and

$$I_3 = I_3^* = 0.5\left(\frac{0.5\,E}{R + 0.5R}\right)$$

Now the effect of these currents can be added. The current through the middle resistance equals $(I_2 - I_2^*)$ which equals zero. Therefore the flux in the middle leg of the E-core cancels. The current flowing through the upper resistance equals,

$$I_1^* + I_3 = \frac{E}{2.0R}$$

Similarly the current flowing through the lower resistance equals,

$$I_1 + I_3^* = \frac{E}{2.0\,R}$$

The flux circulating in the outer legs of the E-core is,

$$\emptyset = \frac{MMF}{2.0\,Rel} = \frac{NI}{2.0\,Rel}$$

So the inductance,

$$L = \frac{N^2 u_o A_c}{2.0\,g}$$

This is an interesting result since it is the same as the result that was derived for the C-core case (both had the same total number of turns, N). The flux produced by the two windings cancels in the middle leg of the E-core and does not add inductance to the magnetic circuit. This effectively makes the E-core behave as a C-core.

Considering the other E-core winding configuration.

Case 2.

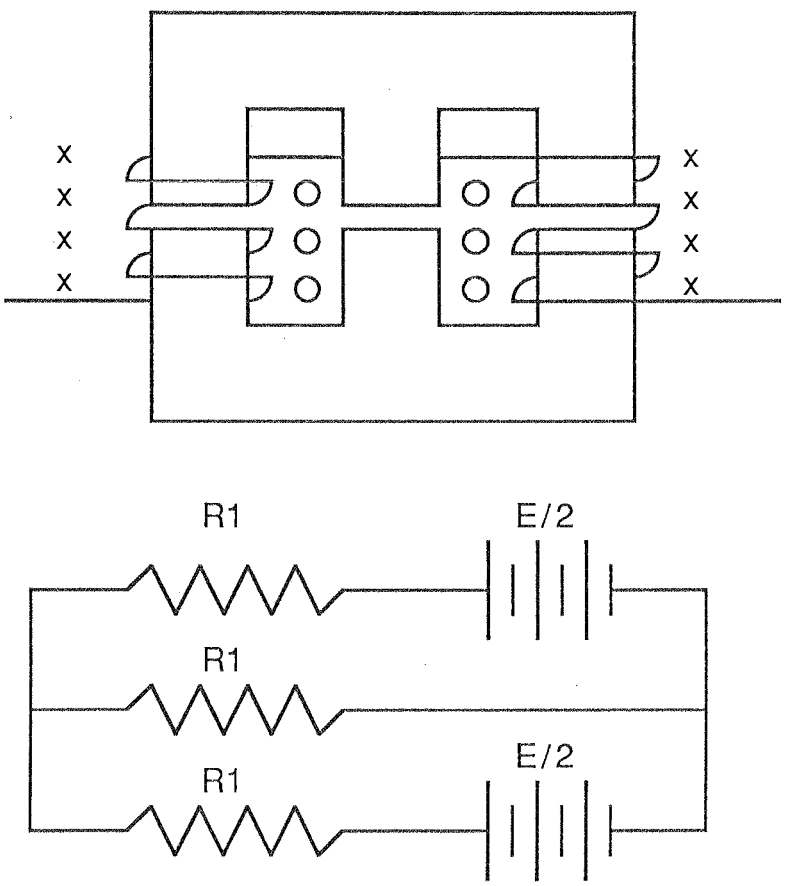

Figure B.4: Two Windings, Arrangement 2.

Each of the windings has N/2 turns. Superposition was applied to the electrical circuit in the same manner as before. The current through the middle resistance was found to be,

$$I = \frac{E}{3.0\,R}$$

The current through the upper and lower resistances are,

$$I = \frac{E}{6.0\,R}$$

Therefore the circulating flux flowing through the E-core due to passing a current through the N turns,

$$\emptyset = \frac{NI}{6.0\,R}$$

and the inductance of the configuration,

$$L = \frac{N^2 u_o A_c}{6.0\,g}$$

which is a third of the inductance value that was derived for the other E-core winding arrangement, Case1. Therefore to achieve a maximum inductance value with an E-core magnetic circuit the winding configuration of Case 1 should be used.

Bibliography.

1.) Colonel Wm.T. McLyman,
'Transformer and Inductor Design Handbook.'
Chapters 2,3,7 & 8.

2.) Electronics Australia,
Vol.44 No.5 May 1982.
'Low Power 12-240 Volt Inverter.'
Pages 61-70.

Vol.47 No.9 Sept. 1985.
'Protected 12-230 Volt 300 VA Inverter.'

3.) R.N.Ivory,
' A Solar Powered 50 Hz DC to AC Inverter.'
Nov. 1989.

4.) F. Langford-Smith,
'Radiotron Designer's Handbook.'
Chapters 5 &10.

5.) Cyril W. Lander,
'Power Electronics'
Chapters 1,5 & 7.